九州大学大学院総合理工学報告
第30巻　第3号　383-388頁　平成20年12月

Engineering Sciences Reports, Kyushu University
Vol. 30, No. 3, pp. 383-388, DEC. 2008

Performance Evaluation of Maxsorb III-1,1,1,2 Tetrafluoroethane Based Adsorption Cooling Cycle

Khairul HABIB[*1] Bidyut Baran SAHA[*2,†] Anutosh CHAKRABORTY[*2]
Ibrahim Ibrahim El-SHARKAWY[*2] and Shigeru KOYAMA[*2]
[†]E-mail of corresponding author: *bidyutb@cm.kyushu-u.ac.jp*

(Received October 31, 2008)

This article presents the transient analysis of a two-bed adsorption chiller using Maxsorb III-1,1,1,2 tetrafluoroethane (HFC-134a) as the adsorbent-refrigerant pair. The simulation has been performed with experimentally confirmed adsorption isotherms, kinetics and isosteric heat of adsorption data. Pertaining a thermodynamically equlibrium model, the performance of the two-bed adsorption cooling cycle has been studied. The cooling capacity and the coefficient of performance (COP) of the cycle have been evaluated also.

Key words: *Maxsorb III, Adsorption isotherms, HFC-134a, Performance evaluation*

1. Introduction

Over the past few decades, thermally powered adsorption cycles have achieved great interests as they appear to be promising from the view point of green house gas emissions and ozone layer depletion problems. Chlorofluorocarbons (CFC) have been identified as the major contributors to the environmental hazard. Adsorption cooling cycles are considered as environmentally benign, having zero ozone depletion potential (ODP) due to the use of natural refrigerants or altrenative refrigerants of CFCs, HCFCs or HFCs. The other advantages of adsorption refrigeration systems are that they are free of vibration as they do not have any moving parts, simple control and lower operation costs.

Generally, the performance of the adsorption chiller depends on the adsorption isotherms, kinetics and isosteric heat of adsorption of the assorted adsorbent-refrigerant pair. A considerable number of experimental and theoretical investigations have been performed on various adsorption system configurations and mathematical modeling of the steady state and transient behavior of adsorption cycles. A certain number of adsorbent-refrigerant pairs have been tested theoretically and experimentally to evaluate the performance of adsorption chiller. Adsorption cooling systems can be operated in both partial vacuum and pressurized conditions. Of the adsorbent-refirigerant pairs working at subatmospheric conditions are silica gel-water, zeolite-water, activated carbon-methanol, and activated carbon fiber-ethanol[1-10]. Several other studies have been performed to investigate the possibility of using different adsorbent-refrigerant pairs for pressurized cooling systems. Adsorption cooling cycles applying activated charcoal-1,1,1,2 tetrafluoroethane (HFC-134a) have been conducted by some researchers[11-15]. The reason for choosing HFC-134a as refrigerant that it is proven to be environmental friendly. In order to save stratospheric ozone layer damaged by chlorofluorocarbons (CFCs), HFC-134a (1,1,1,2-tetrafluoroethane) has been introduced for the purpose of refrigeration. HFC-134a is currently regarded as an exellent replacement for refrigeration due to its no ozone depletion potential (ODP) and global warming potential (GWP).

From the above perspective, the present study deals with the performance investigation of a two-bed Maxsorb III-HFC-134a adsorption chiller. A cycle simulation computer program of the assorted adsorbent-refrigerant pair have been developed to analyze the cooling capacity and COP variations by varying heat transfer

*1 Department of Energy and Environmental Engineering, Graduate student
*2 Department of Energy and Environmental Engineering

fluids (hot and cooling water) inlet temperatures and adsorption/desorption cycle time.

2. Working principle of adsorption chiller

The schematic diagram of the two bed Maxsorb III-HFC-134a adsorption chiller is shown in the Fig. 1. The chiller comprises of four heat exchangers namely evaporator (eva), condenser (cond) and two sorption elements (HX1 and HX 2). The cycle has four valves namely V1, V2, V3 and V4. As shown in Fig. 1, when valves V1 and V3 are opened, valves V2 and V4 are closed. Evaporator and HX 1 is in adsorption process and condenser and HX 2 is in the desorption process. In the adsorption-evaporation process which takes place at pressure P_{eva}; refrigerant in the evaporator is evaporated at evaporation temperature, T_{eva}; and seized heat, Q_{chill} from chilled water. The evaporated vapor is as adsorbed by Maxsorb III which is in the HX1 and cooling water removes the adsorption heat $Q_{ads.}$ The desorption-condensation process takes place at pressure $P_{cond.}$. The desorber (HX 2) is heated to the desorber temperature T_{des} which is provided by the driving heat source Q_{des}. The resulting refrigerant vapor is cooled down to temperature T_{cond} in the condenser by cooling water, which removes condensation heat, Q_{cond} and the warm condensate is refluxed back to the evaporator through a pressure reduction valve to maintain pressure difference between the condenser and the evaporator. Pool boiling is affected in the evaporator by the vapor uptake at the adsorber, and thus completing the refrigeration closed loop or cycle. When the refrigerant concentrations in the adsorber and desorber are at or near their equilibrium levels, the cycle is continued by changing into a short durations (50 s) named pre-heating or pre- cooling, where all refrigerant valves remain closed. When the pressures of desorber and adsorber are nearly equal to the pressures of condenser and evaporator, respectively, then valve between HX 2 and evaporator as well as the valve between HX 1 and condenser is opened to flow the refrigerant.

3. Mathematical modeling

3.1 Adsorption isotherms

To estimate the adsorption uptake of Maxsorb III-HFC-134a system, Dubinin-Astakhov (DA) isotherm model is used in this study. The numerical values of W_0, E and n have been evaluated experimentally and are 1.66×10^{-3} m^3/kg, 81.6×10^3 J/kg and 1.3 respectively.

$$W = W_o \exp\left[-\left\{\frac{RT}{E}\ln\left(p_s/p\right)\right\}^n\right] \qquad (1)$$

3.2 Adsorption kinetics

In the present chiller model, the rate of adsorption or desorption is governed by linear driving force kinetic equation.

$$\frac{dC}{dt} = 15\frac{D_{s0}\exp\left(-E_a/RT\right)}{R_p^2}\left(C_0 - C\right) \qquad (2)$$

In the eq. 2 the numerical values of D_{s0} and E_a are calculated and are found to be 5.82×10^{-11} m^2/s and 135.7×10^3 J/kg, respectively.

3.3 Isosteric heat of adsorption

The isosteric heat of adsorption is extracted from the experimental isotherms of Maxsorb III/R134a and can be expressed by[9],

$$Q_{st} = h_{fg} + E\left[\ln\left(C_0/C\right)\right]^{1/n} + a\left(\frac{T}{T_c}\right)^b \qquad (3)$$

3.4 Adsorption and desorption energy balance

Using the lumped approach for the adsorption bed, which comprises Maxsorb III, the heat exchanger fins and tubes, the energy balance equation is given by,

$$\left(MC_p\right)_{Total}^{bed}\frac{dT_{bedi}}{dt} = \delta M_{ac}\frac{dC_{bedi}}{dt}(Q_{st}) + \left(\dot{m}_w C_{p,w}\right)\left(T_{w,in} - T_{w,out}\right) \qquad (4)$$

where the flag $\delta = 0$ during switching and $\delta = 1$ during adsorption/desorption cycle operation, i denotes the adsorption/desorption bed. The left hand side of adsorber/desorber energy balance equation (Eq. 4) provides the rate of change of internal energy due to the thermal mass of adsorbent(s) and the refrigerant (HFC-134a) and adsorber /desorber heat exchanger during adsorption and desorption.

The first term on the right hand side of Eq. 4 represents the release of adsorption heat during adsorption processor the input of desorption heat during desorption process. The second term on the right hand side of Eq. 4 defines the total amount of heat released to the cooling water upon adsorption or provided by the hot water for desorption. For a small temperature difference across heating/cooling fluid such as water, the outlet temperature of the source is sufficiently accurate to be modeled by the log mean temperature difference (LMTD) method and it is given by:

$$T_{w,o} = T_{bed,i} + \left(T_{w,in} - T_{bed,i}\right)\exp\left[-\frac{(UA)_{bed,i}}{(\dot{m}C_p)_w}\right] \quad (5)$$

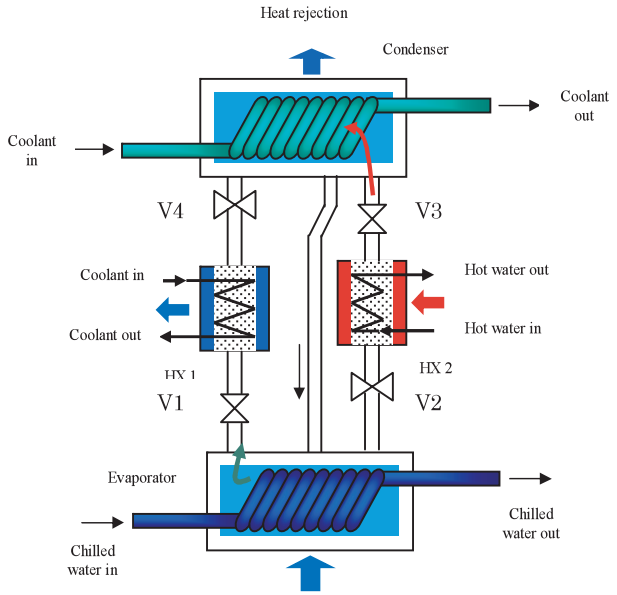

Fig. 1 Schematic diagram of the adsorption chiller.

3.5 Evaporator energy balance

The overall energy balance of the evaporator is dominated mainly by the heat and mass interactions between the evaporator and the adsorption bed. The heat released from the condenser is also taken into account. The energy balance equation of the evaporator can be expressed as,

$$\left(MC_p\right)_{Total}^{eva}\frac{dT_{eva}}{dt} = -\delta h_{fg} M_{ac}\frac{dC_{bed,ads}}{dt} + \dot{m}_{chill} C_{p,chill}\left(T_{chill,in} - T_{chill,out}\right) \quad (6)$$

The left hand side of eq. 6 denotes the change of internal energy due to the sensible heat of liquid refrigerant and the metal of the heat exchanger tubes in the evaporator. On the right hand side, the first term represents latent heat of evaporation for the amount of refrigerant adsorbed; the second term gives the cooling capacity of the evaporator. The chiller water outlet temperature can be written using the log mean temperature difference (LMTD) method as,

$$T_{chill,out} = T_{eva} + \left(T_{chill,in} - T_{eva}\right)\exp\left[-\frac{(UA)_{eva}}{(\dot{m}C_p)_w}\right] \quad (7)$$

3.6 Condenser energy balance

The condenser liquefies the vapor refrigerant coming out from the desorber during desorption and delivers the condensate to the evaporator via pressure reduction valve. It is a water-cooled shell-tube heat exchanger. The energy balance of the condenser can be expressed as,

$$\left(MC_p\right)_{Total}^{cond}\frac{dT_{cond}}{dt} = \delta\left(h_{fg} M_{ac}\frac{dC_{bed,des}}{dt}\right) + \dot{m}_w C_{p,w}\left(T_{w,in} - T_{w,out}\right) \quad (8)$$

The left hand side of eq. 8 defines the rate of change of internal energy of the metallic tubes of the heat exchanger. On the right hand side, the first term represents the latent heat of vaporization due to the amount of refrigerant desorbed during desorption and the amount of heat that the liquid condensate carries away when it leaves the condenser to the evaporator. The last term shows the total amount of heat released to the cooling water. The outlet temperature of the condenser can be expressed using the log mean temperature difference approach,

$$T_{w,out} = T_{cond} + \left(T_{w,in} - T_{cond}\right)\exp\left[-\frac{(UA)_{cond}}{(\dot{m}C_p)_w}\right] \quad (9)$$

The cycle average cooling capacity Q_{chill} and COP are calculated as

$$Q_{chill}^{cycle} = \frac{1}{t_{cycle}}\int_0^{t_{cycle}} (\dot{m}C_p)_{chill}\left(T_{chill,in} - T_{chill,out}\right)dt \quad (10)$$

$$COP = \frac{\int_0^{t_{cycle}} (\dot{m}C_p)_{chill} (T_{chill,in} - T_{chill,out}) dt}{\int_0^{t_{cycle}} (\dot{m}C_p)_{des} (T_{hotwaterin} - T_{hotwaterout}) dt} \quad (11)$$

Here t_{cycle} denotes total cycle time.

5. Results and Discussion

5.1 Chiller transient response

The chiller response with the variation of outlet temperature profiles for heat transfer fluids for Maxsorb III-HFC-134a system is shown in Fig. 2 by using the mathematical models presented herein. Hot and cooling water inlet temperature of the chiller are taken as 80 and 30˚C, respectively. It can be seen from Fig. 2 that the Maxsorb III-HFC-134a cycle is able to reach from transient to nearly steady state within three half cycles or 1800 s, where adsorption/desorption cycle time is taken as 540 s and switching time is taken as 50 s.. The chilled water inlet temperature is taken as 12˚C.

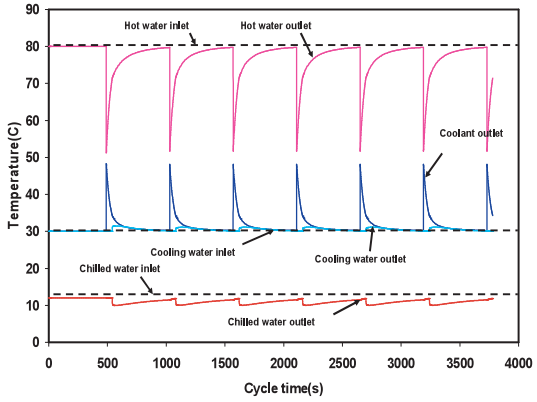

Fig. 2 Outlet temperature of heat transfer fluids of the Maxsorb III-HFC-134a adsorption chiller for rated conditions.

5.2 Adsorption/desorption cycle time

Fig. 3 shows the simulated results of cooling capacity and COP variations with adsorption/desorption cycle time for the assorted adsorbent-refrigerant pair for standard operating conditions of heat transfer fluid temperatures (hot water and chilled water inlet). The hot water and chilled water inlet temperatures have been taken as 80 and 12°C. The switching (preheating and precooling) time is considered as 50 s. It is observed from Fig. 3 that the maximum cooling capacity is around 2.52 kW for the cycle time between 360 to 420 s. It can also be seen that the cooling capacity after reaching the peak point, starts decreasing abruptly. It is also visible from Fig. 3 that COP increases uniformly with the longer adsorption/desorption cycle time and after reaching a certain value (around 600 s) it becomes steady. This is due to the fact that the lower consumption of driving heat allows longer duration cycles. The optimum value of cycle time for COP is 540 s. The optimum COP value is 0.21 when the cycle time is around 550 s.

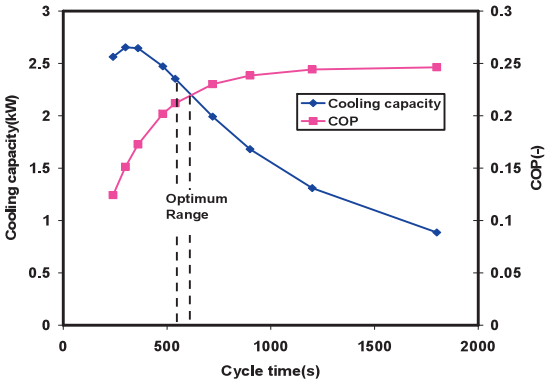

Fig. 3 Effect of cycle time on cooling capacity and COP.

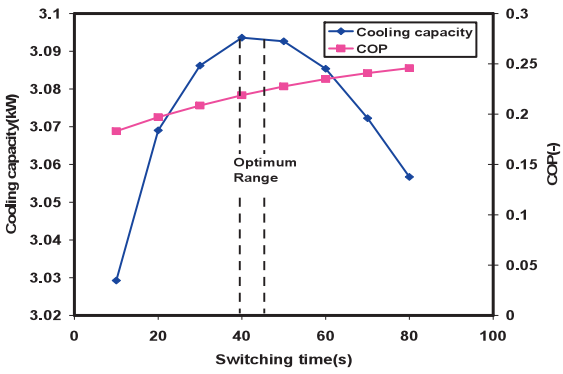

Fig.4 Effect of switching time on cooling capacity and COP.

5.3 Switching time

The switching time has always been an indispensable part of adsorption chiller operation. But rather than immediately connect the saturated cold bed to the condenser, and the regenerated hot bed to the evaporator, a period of isolated, near-isosteric thermal swing is necessary. The condensing will not be hampered if the saturated cold bed is immediately connected to the condenser as the condensate in the condenser can

evaporate and easily maintain the saturated pressure. But a premature connection between the regenerated hot bed and the evaporator would translate into momentary desorption of adsorbed refrigerant and undesirable reduction in instantaneous cooling power. The variation of cooling capacity and COP with the switching time is shown in Fig. 4. It is observable from Fig. 4 that the cooling capacity increases with the increase of switching time until 50 s and reaches a peak point value from 50 to 60 s and after that cooling capacity decreases. It is also visible from Fig. 4 that the COP increases steadily and reaches a maximum value of around 0.25. The optimum value of COP is 0.23 when the switching time is about 60 s.

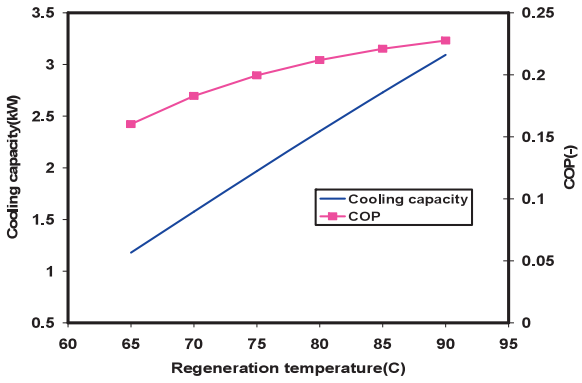

Fig. 5 Variation of cooling capacity and COP with regeneration temperature.

5.4 Regeneration temperature

The effects of regeneration temperature on cooling capacity and COP are shown in Fig. 5 with fixed cooling water and chilled water inlet temperature. Heat transfer fluid flow rates and cycle times are taken as rated values and shown in Table 1. It is clear from Fig. 5 that cooling capacity increases linearly from 1.0 to 3.0 kW with heat source temperature increases from 65 to 90°C. This is due to the fact that the amount of refrigerant circulation increases when the amount of desorbed refrigerant increases with the higher driving heat source temperature.
It is also noticeable from Fig. 5 that COP rises with the rise of regeneration temperature and reaches a peak value of around 0.23 when the regeneration is between 80 to 85°C. The lower value of COP for hot water inlet temperature between 65 to 75°C indicates lower cooling capacity.

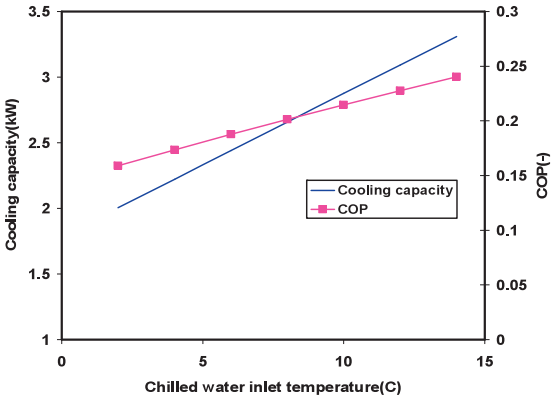

Fig.6 Effect of chilled water inlet temperature on cooling capacity and COP.

5.5 Chilled water inlet temperature

The effect of chilled water inlet temperature on cooling capacity and COP is shown in Fig. 6 with fixed hot and cooling water inlet temperature. Adsorption/desorption cycle time and switching time have been taken as 540 and 50s, respectively. It is observable from Fig. 6 that both the cooling capacity and COP increase linearly with the increase of chilled water inlet temperature.

6. Conclusions

The performance of a two-bed Maxsorb III-HFC-134a based adsorption cooling system has been evaluated in this study. The adsorption isotherms and isosteric heat of adsorption data have been evaluated experimentally by using desorption method. Dubinin-Astakhov (DA) isotherm model is applied to fit the experimental data. The cooling capacity and COP of the assorted adsorbent-refrigerant pair has been calculated in terms of cycle time, switching

Table 1 Rated operating conditions

Hot water inlet		Cooling water inlet		Chilled water inlet	
Temperature(C)	Flow rate(kg/s)	Temperature(C)	Flow rate (ads+cond)(kg/s)	Temperature(C)	Flow rate(kg/s)
80	1.5	30	(1.5+1.5)	12	0.5
Adsorption/desorption cycle time: 540s		Switching time: 50 s			

time, regeneration temperature and chilled water inlet temperature. The amalgamation of Maxsorb III-HFC-134a with Maxsorb III-R507A based cooling cycles can be used as cascading cycle where Maxsorb III-HFC-134a acts in the top cycle and Maxsorb III-R507A works in the bottom cycle. This cascade cycle can be a suitable means for refrigeration application.

Nomenclature

A	area	m^2
COP	coefficient of performance	--
C_p	specific heat capacity	J/kgK
D_{so}	pre-exponential constant	m^2/s
E_a	activation energy	J/kg
h	enthalpy	J/kg
R_p	fiber radius	m
M	mass	kg
$\dot{m}$	mass flow rate	kg/s
Q	power	W
Q_{st}	isosteric heat of adsorption	J/kg
R	universal gas constant	J/kgK
U	overall heat transfer coefficient	W/m^2K
E	characteristic energy	J/kg
P	pressure	Pa
P_s	saturation pressure	Pa
W	instantaneous uptake	m^3/kg
W_0	equilibrium uptake	m^3/kg
n	heterogeneity constant	--
a & b	constants of eq. 3	

Supercripts

bed	sorption heat exchanger
cond	condenser
eva	evaporator

Subscripts

ac	activated carbon
ads	adsorption
chill	chilled water
f	liquid phase
g	gaseous phase
i	adsorption or desorption
w	water
out	outlet
in	inlet

References

1) B.B. Saha et al.,Appl. Phys. Lett., 91 (2007) 111902.
2) B.B. Saha et al., Int. J. Multiphase Flow, 29(8) (2003) 1249.
3) B.B. Saha et al., Int. J. Refrigeration, 26(7) (2003) 749.
4) H.T. Chua et al., Int. J. Refrigeration, 22(3) (1999) 194.
5) L.Z. Zhang et al., Appl. Therm. Eng., 19(2) (1999) 195.
6) L.Z. Zhang et al.,Energy, 24(7)(1999) 605.
7) R.E. Critoph, Solar Energy, 41(1) (1988) 21.
8) R.E. Critoph, Appl. Therm. Eng., 18(9-10) (1998) 799.
9) B.B. Saha et al., Int. J. Refrigeration,30(1) (2007) 86.
10) B.B. Saha et al., Int. J. Refrigeration,30(1) (2007) 96.
11) S.H. Lin et al., J. Environ. Sci. Health, A34(1) (1999) 183.
12) B.S. Akkimaradi et al., J. Chem. Engg. Data, 46 (2001) 417.
13) S. Savitz et al., J. Phys. Chem. B, 103 (1999) 8283.
14) S.H. Lin et al., J. Environ. Eng., 125(11) (1999) 1048.
15) N.D. Banker et al., Carbon, 42 (2004) 117.